Published in final edited form as:
Genesis. 2009 December ; 47(12): 858–863. doi:10.1002/dvg.20577.

Generation of mouse conditional and null alleles of the type III sodium-dependent phosphate cotransporter *PiT-1*

Maria H Festing, **Mei Y Speer**, **Hsueh-Ying Yang**, and **Cecilia M Giachelli***
Department of Bioengineering, University of Washington, Seattle, WA 98195-5061, USA

Abstract

Accelerated vascular calcification occurs in several human diseases including diabetes and chronic kidney disease (CKD). In CKD patients, vascular calcification is highly correlated with elevated serum phosphate levels. *In vitro*, elevated concentrations of phosphate induced vascular smooth muscle cell matrix mineralization, and the inorganic phosphate transporter-1 (PiT-1), was shown to be required. To determine the *in vivo* role of PiT-1, mouse conditional and null alleles were generated. Here we show that the conditional allele, *PiT-1*^{flox}, which has *loxP* sites flanking exons 3 and 4, is homozygous viable. Cre-mediated recombination resulted in a null allele that is homozygous lethal. Examination of early embryonic development revealed that the *PiT-1*$^{\Delta e3,4/\Delta e3,4}$ embryos displayed anemia, a defect in yolk sac vasculature, and arrested growth. Thus, conditional and null *PiT-1* mouse alleles have been successfully generated and PiT-1 has a necessary, non-redundant role in embryonic development.

Keywords

PiT-1; Slc20a1; yolk sac vasculature; anemia; knockout; conditional; mouse; embryonic lethal; type III sodium-dependent phosphate cotransporter

Inorganic phosphate (P_i) is required for cells, and as a negatively-charged anion, must be actively transported into the cell. The highly-homologous and ubiquitously-expressed transmembrane type III sodium-dependent inorganic phosphate transporters (PiT) PiT-1 (also called Slc20a1 or Glvr-1) and PiT-2 (also called Slc20a2 or Ram-1) are proposed to have a general “housekeeping” function of transporting P_i into cells (reviewed in Collins, *et al.*, 2004). Inorganic phosphate additionally plays a role in diseases where ectopic calcification occurs, as fluctuations in mineral metabolisms are risk factors. Hyperphosphatemia is correlated with severe coronary calcification in patients with end-stage renal disease (Shigematsu, *et al.*, 2003; Tomiyama, *et al.*, 2006). Studies into the function of PiT-1 uncovered an essential role in human vascular smooth muscle cell calcification, as cells with reduced PiT-1 levels had reduced susceptibility to phosphate-induced calcification (Li, *et al.*, 2006). Supporting a role for PiT-1 specifically in ectopic calcification, a recent study of Werner Syndrome patients with subcutaneous calcification had overexpression of PiT-1 in their skin (Honjo, *et al.*, 2008). Thus, animal models to examine the physiological and potential pathological role of PiT- 1 are of great interest.

Since there were no available knockout mice of PiT-1, this is the first report of the creation of conditional (*PiT-1*^{flox}) and null (*PiT-1*$^{\Delta e3,4}$) alleles in the mouse model. Here we describe the generation of a murine *PiT-1* conditional allele with *loxP* sites flanking exons 3 and 4, allowing for the conditional deletion of these exons by Cre recombinase. The mouse PiT-1

* Correspondence to: Cecilia M Giachelli, Department of Bioengineering, Box 355061, Seattle, WA 98195-5061, USA, ceci@uw.edu.

gene consists of eleven exons and spans over 12.8 kb. Ten of these eleven exons code for a protein of 681 amino acid residues and has at least ten transmembrane domains (Boyer, *et al.*, 1998). Amino acid residues critical for P_i transport have been determined for PiT-2 and include D28, E68, S113, D506, E575, and S593 (Bøttger and Pedersen, 2002; Bøttger and Pedersen, 2005; Salaün, *et al.*, 2004); these sites are conserved in PiT-1 and thus, would also be predicted to be critical for P_i transport. Removal of exons 3 and 4 in the PiT-1 gene results in a shift in the protein reading frame after position 116 and the creation of an early stop codon after position 120; this truncation removes four of the six residues involved in P_i transport and 83% of the full-length protein. Thus, this *PiT-1* recombined allele is predicted to be a null allele.

To generate the conditional allele of *PiT-1*, a targeting vector was constructed where a *loxP* site was placed upstream of exon 3 and a *pGK-gb2*-neomycin (*Neo*) resistance cassette flanked by *loxP* and *FRT* sites was placed downstream of exon 4, with *Neo* being in opposite orientation to the PiT-1 reading frame: this is the *PiT-1*$^{flox\text{-}neo}$ allele (Fig. 1a). The targeting vector was linearized and electroporated into iTLBA1 mouse embryonic stem (ES) cells and neomycin-resistant colonies were screened via PCR for confirmation of correct targeting of the short and long homology arms (Fig. 1b and c, respectively). Though a number of ES cell colonies had recombination of the short homology arm (Fig. 1b), not all had recombination of the long arm (clones 112 and 311) (Fig. 1c). Two clones that had recombination of both arms (clones 111 and 221) were selected for microinjection and produced chimera offspring. Germline transmission of the conditional allele *PiT-1*$^{flox\text{-}neo}$ from clone 111 was confirmed by PCR screening (data not shown).

The *PiT-1*$^{+/flox\text{-}neo}$ mouse was bred to a FLP1 mouse line to remove the *Neo* cassette via the *FRT* sites and generated the *PiT-1*^{flox} allele in somatic and germ tissue. *PiT-1*^{flox} heterozygous animals were bred and wildtype (WT), heterozygous, and homozygous progeny were produced at Mendelian ratio (Table 1). PCR analysis using primers that flank the *loxP* sites were able to detect the 3′ insertion and removal of the *Neo* cassette leaving the 5′ *loxP* site and a *FRT* site (Fig. 2a and b). Mice heterozygous and homozygous for the conditional allele were viable, healthy, fertile, and grossly indistinguishable from wildtype littermates. Both of the *loxP* sites are functional, as exposure to Cre recombines the allele into the null allele (data not shown).

The *PiT-1*$^{+/flox\text{-}neo}$ mouse was additionally bred to a Cre mouse line to produce the *PiT-1*$^{\Delta e3,4}$ allele in somatic and germ tissues. *PiT-1*$^{\Delta e3,4}$ heterozygous mice were bred, but only WT and heterozygous progeny were born; the absence of PiT-1 null offspring was statistically significant ($p<0.0001$) (Table 1). PCR analysis confirmed removal of exons 3 and 4 (Fig. 2a and c) in the heterozygous mice, and they were viable, healthy, fertile, and grossly indistinguishable from wildtype littermates. Because homozygous null mice were not observed at weaning or as neonates, it was necessary to analyze the embryos to confirm that the null progeny were being created, and to determine the cause of lethality.

PCR analysis of early embryonic stages confirmed that *PiT-1* homozygous null progeny were being produced (Fig. 3a). Semi-quantitative RT-PCR using primers that amplify only exons 3 and 4 did not detect transcript in the null embryos (Fig. 3b, top panel). Primers in exons 2 and 5 amplified a truncated *PiT-1* transcript product lacking exons 3 and 4 (exon 2/5) only in tissues that had the null allele, and the larger wildtype product (exon 2-5) in tissues that had a wildtype allele (Fig. 3b, middle panel). Thus, the null embryos do not express wildtype mRNA, only the truncated transcript from the null allele.

Wildtype, *PiT-1*$^{+/\Delta e3,4}$, and *PiT-1*$^{\Delta e3,4/\Delta e3,4}$ embryos were observed at Mendelian ratios during early embryonic stages (Table 2); after embryonic day (E) 14.5, the absence of

PiT-1$^{\Delta e3,4/\Delta e3,4}$ embryos became statistically significant (p=0.02) and thus, the null genotype was lethal past mid-gestation. Analysis of *PiT-1*$^{\Delta e3,4}$ homozygous embryos reveled an abnormal phenotype beginning at E10.5. The embryos all appeared phenotypically normal (Fig. 3c); however, in a portion of the homozygous nulls, a defect in the vasculature system of the yolk sac could be observed (Fig. 3d). These abnormal yolk sacs had a decrease in the superficial vasculature and appeared severely anemic. By E12.5, the *PiT-1*$^{\Delta e3,4}$ homozygous embryos displayed significant growth retardation and anemia as compared to wildtype littermates (Fig. 3e). In addition, an abnormal yolk sac vasculature was observed in all homozygous null yolk sacs at this time point (Fig. 3f). Lack of erythroid cells and a mature vasculature system to bring nutrients and oxygen to the embryo is incompatible with life since the embryos have developed pass the stage where these requirements could have been obtained by diffusion. Thus, we speculate that the anemia and vascular defects in the *PiT-1*$^{\Delta e3,4/\Delta e3,4}$ embryos leads to hypoxia and nutrient-deprivation, growth arrest, and lethality. Consistent with this, null embryos were observed resorbing at E12.5 (Fig. 3e, far left) and were completely resorbed after E14.5 (Table 2). The observation that these embryos were not resorbing at the same developmental stage could be due, in part, to the mixed strain background these mice were on. All wildtype and heterozygous embryos analyzed were developmentally normal, consistent with observing the expected number of these progeny at weaning (Table 1).

Changes in mRNA expression level of the other type III sodium-dependent phosphate transporter PiT-2 was assayed to determine if *PiT-2* expression increased to compensate for the loss of wildtype *PiT-1* mRNA in the null progeny. There was no observed increase in *PiT-2* transcript when comparing null and wildtype yolk sacs (Fig. 3g, left) or embryos (Fig. 3g, right) at E10.5 (when phenotypes were observed only in the yolk sac) and E11.5 (when phenotypes were observed in both the yolk sac and embryo). These results indicate that loss of exons 3 and 4 in the *PiT-1* gene results in a null allele with an embryonic lethal phenotype. PiT-1 is thus necessary for embryonic development, and is non-redundant, as PiT-2 could not compensate for the loss of PiT-1 and allow development into adulthood.

The *PiT-1* conditional allele provides a useful tool to study the tissue-specific effects of removing a ubiquitous sodium-dependent phosphate cotransporter. Considering the role PiT-1 plays in matrix calcification *in vitro*, effects on the *in vivo* calcification of normal bone development can be studied, along with the effects of PiT-1 loss in mouse vascular calcification models. Use of temporal-specific control of Cre expression will allow for the ability to study the function of PiT-1 later in development and in adulthood in the vasculature system.

Methods

Generation of the *PiT-1* Alleles

Briefly, the targeting vector for the *PiT-1* gene was constructed by ligating a 9.8 kb region from a C57BL/6 BAC clone (RPCI23) into a 2.4 kb backbone vector (pSP72, Promega). The short homology arm extended 1.5 kb downstream of exon 4, while the long homology arm extended 7.6 kb upstream of exon 3. A single *loxP* site was inserted on the 5′ side of exon 3, while a *pGK-gb2 loxP/FRT Neo* cassette in opposite orientation to the *PiT-1* reading frame was inserted on the 3′ side of exon 4. The 14 kb targeting vector was linearized and electroplated into iTLBA1 mouse embryonic stem cells (C57BL/6 × 129SvEv hybrid) (Ingenious Targeting Labs, Inc., Stonybrook, NY); after G418 antibiotic selection, targeting was confirmed via PCR screening which used primers (Table 3) LAN1/A3 to produce a 2.4 kb targeted product, and LOX1/SDL2 to produce 389 bp WT and 453 bp targeted product. Two independent recombinant clones (111 and 221) were microinjected and a single male chimera from clone 111 was produced and had germline transmission of the targeted

conditional allele PiT-1$^{flox\text{-}neo}$. The *PiT-1*$^{+/flox\text{-}neo}$ male mouse was bred to the FLP1 recombinase mouse line (*B6;SJL-Tg(ACTFLPe)9205Dym/J*; The Jackson Laboratory, Bar Harbor, ME) to generate the *PiT-1*^{flox} allele. The same male was bred to a Cre recombinase mouse line (*Tg(Sox2-cre)1Amc/J*; The Jackson Laboratory, Bar Harbor, ME) to produce the *PiT-1*$^{\Delta e3,4}$ allele. Strain background was not purified after these matings, so mice were on a mixed background of 129SvEv and C57BL/6 for the *PiT-1*^{flox} allele, and 129SvEv;C57BL/6;CBA;DBA/2 for the *PiT-1*$^{\Delta e3,4}$ allele. These mice were housed under pathogen-free conditions and all experiments complied with policies and protocols of the IACUC of the University of Washington.

Genotyping

Genotyping of the mice was performed using PCR of DNA extracted from tail biopsies using the HotSHOT method (Truett, *et al.*, 2000). Genotyping of embryos was performed on extraembryonic tissue incubated in lysis buffer (60mM Tris, pH8.0 and 0.5mg/mL proteinase K) overnight at 60°C. Proteinase K was heat-inactivated at 95°C for 15 minutes and the solution was used without further extraction. Detection of the various alleles use the primers (Operon) listed in Table 3. PCR reactions were performed for 35 cycles of 95°C for 30 seconds, 58°C for 1 minute, and 72°C for 1 minute using GoTaq Flexi DNA polymerase (Promega). Primers CreY-1/CreY-2 amplify a 350 bp product from *Cre*, FLPF/FLPR amplify a 725 bp product from *FLP1*, Ex2F/Ex3R amplify 424 bp WT and 488 bp conditional allele products, Ex4F/int4R3 amplify 268 bp WT and 430 bp conditional allele products, and Ex2F/int4R3 amplify a 504 bp recombined product under these PCR conditions. Primers Ex2F, Ex3R, int4R3, and Ex4F were designed using the Primer3 program (Rozen and Skaletsky, 1998).

Embryo Analysis

Embryos were obtained from timed pregnancies (day of vaginal plug was considered E0.5) and were dissected free of maternal tissues in 1× phosphate buffered saline (PBS), pH7.4. Gross evaluations of embryos were performed using a SZ40 Stereozoom microscope (Olympus) and pictures were taken using a CoolPix 990 digital camera (Nikon) with mounting adapter. Images were processed using Photoshop Elements v5.0 (Adobe Systems, Inc.).

Statistical Analysis

P-values were calculated via a chi-squared test with a two-tailed distribution using GraphPad Prism v5.02 (GraphPad Software, Inc.). P-values less than 0.025 were considered statistically significant.

RNA Analysis

Embryonic and yolk sac tissue was flash-frozen on dry ice and total RNA extracted using TRIzol (Invitrogen) according to manufacturer's protocol. Up to 2 μg of DNaseI-treated RNA was used to make cDNA using pdN6 random hexamer primers (Operon) with the Omniscript RT kit (QIAGEN) following manufacturer's protocol. Primers PiT-1exon3/PiT-1exon4 amplify a 120 bp WT cDNA transcript, PiT-1exon2/PiT-1exon5 amplify a 507 bp WT and a 208 bp truncated cDNA transcript, PiT-2 F/PiT-2R amplify a 179 bp cDNA transcript, and 18S F/18S R amplify a 350 bp cDNA transcript using the PCR conditions mentioned above and 30 cycles. PiT-1 and PiT-2 primers were designed using the Primer3 program (Rozen and Skaletsky, 1998).

Acknowledgments

The authors thank Dr. Xianwu Li for assisting in the design of the targeting strategy and Elizabeth Leaf for assistance in maintaining the mouse colony. Primer3 program includes software developed by the Whitehead Institute for Biomedical Research. This work was supported by grants NIH HL07828 (MHF) and HL62329 (CMG).

References

Bøttger P, Pedersen L. Two highly conserved glutamate residues critical for type III sodium-dependent phosphate transport revealed by uncoupling transport function from retroviral receptor function. J Biol Chem. 2002; 277(45):42741–42747. [PubMed: 12205090]

Bøttger P, Pedersen L. Evolutionary and experimental analysis of inorganic phosphate transporter PiT family reveals two related signature sequences harboring highly conserved aspartic acids critical for sodium-dependent phosphate transport function of human PiT2. FEBS. 2005; 272:3060–3074.

Boyer CJC, Baines AD, Beaulieu É, Béliveau R. Immunodetection of a type III sodium-dependent phosphate cotransporter in tissues and OK cells. Biochemica et Biophysica Acta. 1998; 1368:73–83.

Collins JF, Bai L, Ghishan FK. The SLC20 family of proteins: dual functions as sodium-phosphate cotransporters and viral receptors. Pflugers Arch – Eur J Physiol. 2004; 447:647–652. [PubMed: 12759754]

Honjo S, Yokote K, Fujimoto M, Takemoto M, Kobayashi K, Maezawa Y, Shimoyama T, Satoh S, Koshizaka M, Takada A, Irisuna H, Saito Y. Clinical outcome and mechanism of soft tissue calcification in Werner syndrome. Rejuvenation Res. 2008; 11(4):809–819. [PubMed: 18729813]

Li X, Yang HS, Giachelli C. Role of the sodium-dependent phosphate cotransporter, Pit-1, in vascular smooth muscle calcification. Circ Res. 2006; 98:905–912. [PubMed: 16527991]

Rozen, S.; Skaletsky, HJ. Primer3. 1998. Code available at http://www-genome.wi.mit.edu/genome_software/other/primer3.html

Salaün C, Maréchal V, Heard JM. Transport-deficient PiT2 phosphate transporters still modify cell surface oligomers structure in response to inorganic phosphate. J Mol Biol. 2004; 340(1):39–47. [PubMed: 15184021]

Shigematsu T, Kono T, Satoh K, Yokoyama K, Yoshida T, Hosoya T, Shirai K. Phosphate overload accelerates vascular calcium deposition in end-stage renal disease patients. Nephrol Dial Transplant. 2003; 18(Suppl3):iii86–89. [PubMed: 12771310]

Tomiyama C, Higa A, Dalboni MA, Cendoroglo M, Draibe SA, Cuppari L, Carvalho AB, Neto EM, Canziani ME. The impact of traditional and non-traditional risk factors on coronary calcification in pre-dialysis patients. Nephrol Dial Transplant. 2006; 21(9):2464–2471. [PubMed: 16735378]

Truett GE, Heeger P, Mynatt RL, Truett AA, Walker JA, Warman ML. Preparation of PCR-quality mouse genomic DNA with hot sodium hydroxide and tris (HotSHOT). Biotechniques. 2000; 29(1):52–54. [PubMed: 10907076]

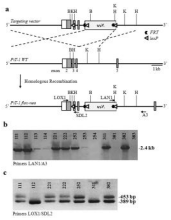

Fig. 1.

Generation of the *PiT-1*$^{flox\text{-}neo}$ allele. (**a**) A genomic sequence (shown to scale) containing exons 2-4 was subcloned for targeting vector construction and a *loxP* site was placed between exons 2 and 3, while a *Neo* cassette (in reverse orientation) flanked with *loxP* and *FRT* sites was placed downstream of exon 4 (top). Recombination with the wildtype locus (middle) produced the targeted allele *PiT-1*$^{flox\text{-}neo}$ (bottom). (**b** and **c**) Homologous recombinants were identified by PCR analysis. (**b**) Primers LAN1 and A3 amplify a 2.4 kb targeted product to detect recombination of the short homology arm. (**c**) Primers LOX1 and SDL2 amplify a 389 bp WT product and a 453 bp targeted product to detect recombination of the long homology arm. Coding exons 2-5 are indicated by grey boxes; non-coding portion of exon 2 indicated by a white box; *loxP* sites indicated with white triangles, *FRT* sites indicated with black chevrons; arrows indicate relative placement of primers; B–BglII, K-KpnI, H-HindIII, WT-wildtype.

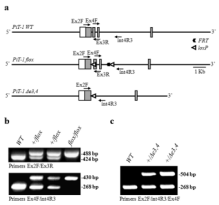

Fig. 2.

Alleles from Cre and FLP-mediated recombination and the PCR strategy used to identify them. (**a**) *WT* (top), *PiT-1*^{flox} (middle), and *PiT-1*$^{\Delta e3,4}$ (bottom) alleles (to scale) and relative placement of the primers (arrows) used to genotype them. (**b**) Genotyping for the *PiT-1*^{flox} allele. Primers Ex2F and Ex3R (top panel) detect the presence (488 bp) or absence (424 bp) of the 5′ *loxP* site. Primers Ex4F and int4R3 (bottom panel) detect the presence (430 bp) or absence (268 bp) of the 3′ *loxP* and *FRT* sites. Breeding of *PiT-1*$^{+/flox}$ mice produce *WT*, heterozygous, and homozygous mice at Mendelian ratios. (**c**) Genotyping for the *PiT-1*$^{\Delta e3,4}$ allele. Primers Ex4F and int4R3 amplify only the *WT* allele (268 bp), and Ex2F and int4R3 amplify the *PiT-1*$^{\Delta e3,4}$ allele (504 bp). Breeding of *PiT-1*$^{+/\Delta e3,4}$ mice produces WT and heterozygous mice, but no homozygous mice. Exons indicated by boxes; *loxP* sites indicated with white triangles, *FRT* sites indicated with black chevrons; WT-wildtype.

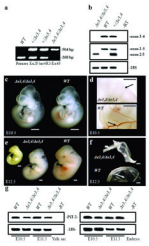

Fig. 3.

Analysis of *PiT-1*$^{\Delta e3,4/\Delta e3,4}$ during embryonic development. (**a**) Genotyping for the *PiT-1*$^{\Delta e3,4}$ allele. Primers Ex2F/int4R3/Ex4F amplify the *WT* allele (268 bp) and the *PiT-1*$^{\Delta e3,4}$ allele (504 bp). Breeding of *PiT-1*$^{+/\Delta e3,4}$ mice produce *WT*, heterozygous, and homozygous embryos. (**b**) Semi-quantitative RT-PCR of E11.5 embryos detects *WT* transcript (exon 3-4) only in tissue with a *WT* allele (top), while *WT* (exon 2-5) and truncated (exon 2/5) transcripts can be detected in embryos that have the *WT* or *Δe3,4* alleles, respectively (middle). Loading control for samples (bottom). (**c**) At E10.5, *PiT-1*$^{\Delta e3,4/\Delta e3,4}$ embryos are indistinguishable from *WT* littermates. (**d**) However, some *PiT-1*$^{\Delta e3,4/\Delta e34,}$ yolk sacs appear anemic and lack the mature vasculature observed in *WT* (arrow). (**e**) At E12.5, *PiT-1*$^{\Delta e3,4/\Delta e3,4}$ embryos are developmentally delayed and anemic as compared to *WT*. (**f**) No mature vasculature was observed in *PiT-1*$^{\Delta e3,4/\Delta e34,}$ yolk sacs compared to *WT* (arrow). (**g**) Semi-quantitative RT-PCR detects no increase of *PiT-2* transcript (top) at E10.5 or E11.5 in yolk sacs (left) or embryos (right) in the homozygous tissue. Loading control for samples (bottom). E-embryonic day, *WT*-wildtype, -RT-no reverse transcriptase control; scale bar = 1mm.

Table 1

Ratio of wildtype (WT), heterozygous, and homozygous offspring at postnatal day (P) 21 from heterozygous matings.

	Genotype Observed [Expected]				
***PiT-1* Allele**	**WT**	**Heterozygous**	**Homozygous**	**Total**	**p[a]**
flox	7[9]	18[16]	9[9]	34	0.71
Δe3,4	32[22]	55[43]	0[22]	87	<0.0001

[a] p-value

Table 2

Ratio of embryos from *PiT-1*$^{+/\Delta e3,4}$ matings at various embryonic (E) stages and the number of abnormal embryos observed.

	Genotype Observed [Expected]						
Stage	***WT***	***+/Δe3,4***	***Δe3,4/Δe3,4***	**Total embryos**	**rs**[a]	**n**[b]	**p**[c]
E10.5	10[13]	27[25]	14[13] (4)[d]	51	2	5	0.63
E11.5	17[12]	19[24]	12[12] (12)[d]	48	1	5	0.21
E12.5	14[12]	23[22]	9[12] (4)[d] (5)[e]	46	8	6	0.57
E13.5	9[8]	16[14]	5[8] (2)[d] (3)[e]	29	4	4	0.46
>E14.5	11[8]	20[16]	1[8] (1)[e]	32	9	5	0.02

[a] number of completely resorbed embryos

[b] number of litters

[c] p-value

[d] number abnormal

[e] number actively resorbing

Table 3

Primers and oligo sequences used in analysis.

Primer name	Oligo Sequence 5′ → 3′
A3	GGGATAGGTAGGGAATGACTAGCC
LAN1	CCAGAGGCCACTTGTGTAGC
LOX1	GGCATTCTCCGTGGGAGCCAATG
SDL2	CGTTCAAAAACGAAGCCACGAGC
Ex2F	CTCATCCTGGGCTTCATCAT
Ex3R	CGGAAGCTTCAAAAACGAAG
int4R3	TTCCTTCCTGAATGCCCTCT
Ex4F	TCTCCGCTGCTTTCTGGTAT
CreY-1	TGCCACGACCAAGTGACAGCAATG
CreY-2	AGAGACGGAAATCCATCGCTCG
FLP F	CACTGATATTGTAAGTAGTTTGC
FLP R	CTAGTGCGAAGTAGTGATCAGG
PiT-1exon2	GTGGGAGCCAATGATGTAGC
PiT-1exon3	TGTATTGTCGGTGCAACCAT
PiT-1exon4	ATACCAGAAAGCAGCGGAGA
PiT-1exon5	CGATTGTGCAGGCATAAAAA
PiT-2 F	CTGTTCCAAACGGTCTCCAG
PiT-2 R	CACGAATAGCCACACGAAGA
18S F	GTTGGTGGAGCGATTTGTCT
18S R	GGCCTCACTAAACCATCCAA